Research Square

Preprints are preliminary reports that have not undergone peer review.
They should not be considered conclusive, used to inform clinical practice,
or referenced by the media as validated information.

Pt-WO x /TiO 2 catalyst for nitrogen oxide to ammonia reaction using H 2 reductant

Chandan Chaudhari

chandan.chaudhari@aist.go.jp

Renewable Energy Advanced Research Center, National Institute of Advanced Industrial Science and Technology (AIST)

Yuichi Manaka

Renewable Energy Advanced Research Center, National Institute of Advanced Industrial Science and Technology (AIST)

Tetsuya Nanba

Renewable Energy Advanced Research Center, National Institute of Advanced Industrial Science and Technology (AIST)

Article

Keywords: NOx abatement, H2 reductant, Ammonia, Platinum, tungsten bronze formation

Posted Date: July 1st, 2026

DOI: https://doi.org/10.21203/rs.3.rs-9551100/v1

License: This work is licensed under a Creative Commons Attribution 4.0 International License.
Read Full License

Additional Declarations: No competing interests reported.

Pt-WO_x/TiO_2 catalyst for nitrogen oxide to ammonia reaction using H_2 reductant

Chandan Chaudhari,[*a] Yuichi Manaka [*a,b] and Tetsuya Nanba[a]

[a]Renewable Energy Advanced Research Center, National Institute of Advanced Industrial Science and Technology (AIST), 2-2-9 Machiikedai, Koriyama, Fukushima, 963-0298 Japan

[b]School of Materials and Chemical Technology, Institute of Science Tokyo, 2-12-1 Okayama, Meguro-ku, Tokyo, 152-8552 Japan

***Corresponding authors**

Chandan Chaudhari and Yuichi Manaka

Email: chandan.chaudhari@aist.go.jp

Email: yuichi.manaka@aist.go.jp

ORCID

Chandan Chaudhari: 0000-0003-1035-3144

Yuichi Manaka: 0000-0001-5872-3365

Tetsuya Nanba: 0000-0002-2098-2430

Abstract

Undoped Pt/TiO_2 and WO_x-doped in Pt/TiO_2 catalysts with varying WO_x contents were examined for the selective conversion of nitrogen oxide to ammonia reaction. Above 150 °C, 5 wt% WO_x-doped Pt/TiO_2 catalyst exhibited the highest ammonia yield (97 %), outperforming the undoped Pt/TiO_2 catalyst (88%). XRD and XPS analysis revealed the tungsten bronzes formation. Pt-5 wt% WO_x/TiO_2 showed moderate lower oxidation (W^{4+}) concentration. CO chemisorption demonstrated strong metal-support interactions (SMSI) which assist in lower oxidation formation as well as ammonia formation.

These findings highlight the potential of WO_x-doped Pt/TiO_2 as an efficient catalyst for NO_x-to-ammonia conversion, particularly in high-temperature regions.

Keywords: NO_x abatement, H_2 reductant, Ammonia, Platinum, tungsten bronze formation,

Abbreviations

NH_3- SCR	NH_3-Selective Catalytic Reduction
NTA	Nitrogen oxide To Ammonia
XRD	X-ray Diffraction
XPS	X-ray Photoelectron Spectroscopy
NH_3-TPD	NH_3-Temperature Programed Desorption
H_2-TPR	H_2-Temperature-Programmed Reduction
SMSI	Strong Metal-Support Interactions (SMSI)

1. Introduction

After the industrial revolution, the global energy sources are mainly focused on combustion of coal and other fossil fuels which are responsible for emission of CO_2 and global warming. Therefore, carbon-free fuels are required to enhance sustainability in power plants and transport sectors. As a Carbon-free fuel, H_2 has gained much attention owing to environmentally friendly byproduct formation (H_2O). H_2 is sustainably produced by water electrolysis in the presence of photovoltaic or wind power generators. Nevertheless, H_2 combustion in air can lead to the formation of nitrogen oxides as byproduct which cause photochemical smog, acid rain, and ozone depletion [1-4]. Therefore, NO_x abatement is required to meet emission standards. Traditionally, NO is converted to N_2 and H_2O using ammonia as reductant which is commonly known as Selective Catalytic Reduction (NH_3- SCR) ($4\ NO + 4\ NH_3 + O_2 \rightarrow 4\ N_2 + 6H_2O$) [5].

In recent years, a new approach has been introduced for the recovery of NO ($ReNO_x$) [6]. In this approach, NO is selectively converted to ammonia using CO-H_2O or H_2 reductant (Nitrogen oxide To Ammonia; NTA) [7-9]. Ammonia is an important feedstock for fertilizers and can be act as energy carrier. The NTA reaction using H_2 reductant is an environmentally friendly way for NO abatement in comparison to CO-H_2O due to zero emission of greenhouse gas (CO_2). However, high selectivity for ammonia is still a challenging task because of the formation of molecular N_2. Few catalytic methods have been reported for NTA reaction. SiO_2- and ZrO_2-supported Pt catalysts have been reported for ammonia synthesis from NO-H_2 [10-12]. Recently, supported platinum and palladium catalysts developed for ammonia formation by Adam group.[11] However, these catalysts suffer from low ammonia selectivity. Therefore, development of catalyst with high ammonia selectivity is required.

The promoter played a vital role in ammonia formation from NO-H_2. In early report, Mergler et al. studied the effect of CoO_x addition on the activity of Pt/SiO_2 for NO-H_2 reaction.[9] Among the tested catalysts, PtCoO_x/SiO_2 catalyst showed high selectivity for ammonia formation. Yu et al. described the promotion effect of Cr on Pt/ZSM-35 catalyst which facilitated NOx adsorption and the generation of NH_x species [13]. Liu et al. examined WO_x promoted Pt/TiO_2 catalysts for H_2-SCR reaction [14]. The synergetic effect between Pt and WO_x assisted H-spillover from Pt to WO_x and TiO_2 which accelerated the interaction between H_2 and adsorbed NO_x. Such synergetic effects have not been studied for nitrogen oxide to ammonia reaction. In this study, we examined the effect of WO_x doping on the activity of Pt/TiO_2 catalyst for nitrogen oxide to ammonia reaction. The physiochemical properties of Pt-WO_x/TiO_2 and Pt/TiO_2 were also investigated.

2. Experimental

2.1 Catalyst preparation

Titanium tetraisopropoxide ($(((CH3)_2CHO)_4Ti$), Ammonium paratungstate pentahydrate ($(NH_4)_{10}W_{12}O_{41.5}H_2O$), WO_3 and hexachloroplatinic(IV) acid hexahydrate ($H_2PtCl_6.6H_2O$) were purchased from FUJIFILM Wako Pure Chemical Co., Ltd. Japan. TiO_2 was prepared by using titanium tetraisopropxide precursor which was described in previous report [9]. The solution of water (20 mL) and ethanol (20 mL) was added to the solution of ethanol (50 mL) and titanium isopropoxide (30 mL) at 50 °C. The solvent was removed by evaporation (oven) at 80 °C for 12 h and calcined in air at 700 °C for 4 h. 1 wt% Pt/TiO_2 catalyst was prepared by impregnation method using H2PtCl6. An appropriate amount (2 g) of TiO_2 was added to aqueous solution (100 mL) of Pt precursor. The solvent was extracted using evaporation under reduced pressure (rotary evaporator). Then, the catalyst was calcined in air at 500 °C for 4 h and followed by reduction in 10% H_2/N_2 flow at 400 °C for 1 h. Similarly, 1 wt% Pt-WO_x/TiO_2 catalyst was synthesized by impregnation method. The amount of W precursor 0.040, 0.195, 0. 0.41, and 0.92 g was used for 1, 5, 10, and 20 wt % catalyst respectively. An appropriate amount of Pt precursor, W precursor and TiO_2 added to 100 mL of deionized water. Then, the mixture was dried by using rotary evaporator, calcined at 500 °C for 4 h, and followed by reduction at 400 °C for 1 h.

2.2 Characterization

The powder X-ray diffraction (XRD) was recorded using RINT Ultima+, RIGAKU diffractometer with a Cu Kα radiation source. X-ray photoelectron spectroscopy (XPS) analysis was carried out using Thermo scientific (K-alpha). The binding energy (BE) of each catalyst was calibrated to C 1s binding energy of 284.6 eV. H_2 temperature-programmed reduction (H_2-TPR) was carried out using BELCAT-II analyzer with a quartz tube reactor. Before the measurement, the catalyst was treated by O_2 at 400 °C for 0.5 h and purged by He. Then, the reactor cooled down to -70 °C in He and treated with 5% H_2/He. The temperature increased by 10 °C/min rate. The amount of CO uptake was

calculated by CO pulse chemisorption at 50 °C using BELMETAL instrument. In standard procedure, the catalyst was oxidized by O_2 at 400 °C for 0.5 h and reduced by H_2 at 400 °C for 0.5 h. Acidic sites of all catalysts were calculated by NH_3-temperature programed desorption (NH_3-TPD). NH_3-TPD experiments carried out using BELCAT II and a quartz tube reactor. The catalyst was pretreated at 500 °C in He for 0.5 h. Then, the catalyst was cooled down to 100 °C and exposed to NH_3 for 0.5 h.

2.3 Catalytic activity measurement

The catalytic activity was measured by using a fixed-bed reactor and 0.15 g of catalyst. The composition of feed gas was 1000 ppm NO and 3000 H_2 in Ar balance with total flow 250 mL/min. NO conversion and NH_3 yield were calculated by Fourier transform IR spectroscopy (iS50, Thermo Fischer) equipped with a multi-reflection gas cell and gas chromatograph (3000 Micro GC, Micron). N_2 was obtained as a byproduct in nitrogen oxide to ammonia reaction. The NO conversion and ammonia yield were calculated by eqn. (1) and (2).

$$\text{NO conversion (\%)} = \frac{[NO]_{inlet} - [NOx]_{outlet}}{[NO]_{inlet}} \times 100\% \quad (1)$$

$$NH_3 \text{ yield (\%)} = \frac{[NH_3]_{outlet}}{[NO]_{inlet}} \times 100\% \quad (2)$$

3. Results and Discussion

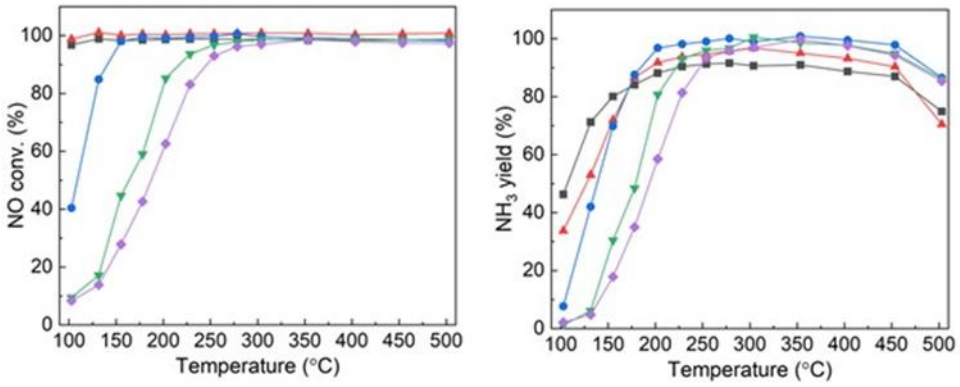

Fig. 1 Effect of temperature on NO conversion (a) and NH_3 formation (b) over undoped Pt/TiO_2 (■), Pt-1 wt% WO_x/TiO_2 (▲), Pt-5 wt% WO_x/TiO_2 (●), Pt-10 wt% WO_x/TiO_2 (▼), Pt-20 wt% WOx/TiO_2 (♦)

Initially, Pt/TiO_2 catalysts with different WO_x loading (0, 1, 5, 10, and 20 wt%) were prepared and investigated for NTA reaction using different temperatures (Fig. 1). Below 155 °C, Pt/TiO_2 showed high activity for NO conversion (99 %) with a Pt/TiO_2 showed high activity for NO conversion (99 %) with ammonia yield (80 %). WO_x-doped Pt catalysts gave relatively low NO conversion and NH_3 formation. When the temperature was raised to 200 °C, 5 wt% WO_x-doped catalyst gave high ammonia yield (97 %). The order of reactivity for ammonia formation was 5 wt% WO_x> 1 wt% WO_x > 0 wt% WO_x > 10 wt% WO_x > 20 wt% WO_x. The activity of Pt/TiO_2 after WO_x-doping was enhanced above 175 °C. However, WO_x-doped catalysts were unable to produce ammonia selectively below 155 °C. This phenomenon can be explained by the hydrogen spillover effect. In previous study, Shun et al. investigated hydrogen spillover effect using TiO_2 or WO_3 supported Ru catalysts [15]. They found that Ru/TiO_2 showed hydrogen spillover on its surface below 50 °C which expanded to the

subsurface in the temperature range of 50 °C - 150 °C. On the other hand, Ru/WO_3 catalyst did not show hydrogen spillover below 50 °C and showed hydrogen spillover in the temperature range of 50-150 °C. In this temperature range, hydrogen atom migrated to bulk instead of WO_x surface.

To understand effect of WO_x loading and catalytic activity, we characterized all catalysts by X-ray diffraction (XRD). As shown in Fig. 2, XRD pattern of Pt/TiO_2 catalyst showed the sharp peaks of anatase and rutile phases. No Pt diffraction peak was observed at 39.8°, suggesting high Pt dispersion in Pt/TiO_2. Next, we compared the commercial WO_3 with unreduced and reduced catalysts to confirm WO_3 formation. XRD pattern of commercial WO_3 showed sharp diffraction peaks at 23.1°, 23.5° and 24.3° were assigned to monoclinic WO_3 [16, 17]. Similarly, the unreduced WO_x doped catalysts showed sharp peaks at 23.1°, 23.5° and 24.3°, indicating the formation of WO_3 (Fig S1). After H_2 reduction, no distinct WO_3 diffraction peaks observed, suggesting that the WO_x phase was amorphous or highly dispersed (Fig 2) [18].

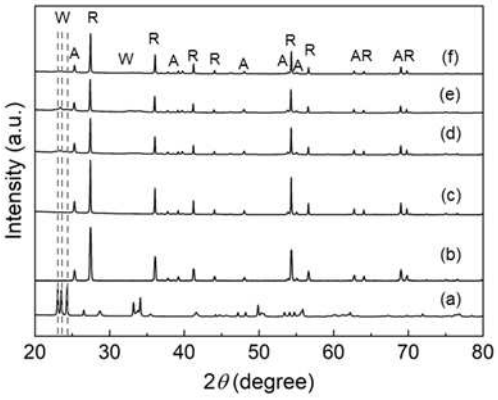

Fig. 2 XRD analysis of commercial WO_3 (a) and reduced catalysts; Pt/TiO_2 (b), Pt-1 wt% WO_x/TiO_2 (c), Pt-5 wt% WO_x/TiO_2 (d) Pt-10 wt% WO_x/TiO_2 (e) and Pt-20 wt% WO_x/TiO_2 (f). Abbreviation: A, anatase; R, rutile; W, WO_3

We analyzed WO_x-doped Pt/TiO_2 catalysts to confirm W reduction, by X-ray photoelectron spectroscopy (XPS). Fig. S2 shows two peaks from W 4f which were fitted to $4f_{7/2}$ and $4f_{5/2}$. These broad peaks at 35.5 and 37.5 eV were assigned to WO_3 (W^{6+}) [19, 20]. After the peak deconvolution, W^{6+} state was found to co-exist with W^{5+} and W^{4+} oxidation states. The peaks related to W^{5+} appeared at 33.7 and 36.6 eV [20]. Over reduced W^{4+} state showed peaks at 32.9 and 34.2 eV [22]. The satellite peak associated with W-O-Ti were observed at 39.1 and 40.5 eV [19]. Furthermore, the degree of W reduction was different in every catalyst. When W amount in the catalyst was increased, the degree of W reduction also increased (Table S1). The order of W reduction was 1 wt% (5 %) < 5 wt% (6 %) < 10 wt% (9 %) < 20 wt% (12 %). Previous study speculated that the reduction of W occurred in the presence of Pt [23-25]. Initially, hydrogen molecules are dissociated with hydrogen atoms on Pt sites which spill over to neighboring WO_3 and lead to the formation of tungsten bronzes (H_xWO_3). The formation of tungsten bronzes may be a crucial factor in low temperature NTA reaction. Highly reduced catalysts (5, 10, or 20 wt% WO_x) gave low ammonia yield below 175 °C. The Hydrogen available in the presence of these catalysts was likely used to tungsten bronzes formation rather than ammonia formation. In contrast, less reduced W catalysts (1 wt% WO_x) employ available hydrogen for ammonia formation instead of tungsten bronzes formation. In high temperature region (> 275 °C), all WO_x-doped catalysts have higher yield than undoped catalyst (Pt/TiO_2). This phenomenon might be attributed to hydrogen release from the tungsten bronzes which might be useful NTA reaction [26].

Next, we investigated W reducibility, Pt-W interactions and H_2 consumption by H_2-temperature programmed reduction (H_2-TPR). As shown in Fig. 3, TPR profile of TiO_2 showed a broad peak in the temperature range of 300-700 °C with peak maximum at 600 °C with small H_2 consumption (0.022 mmol/g). 5 wt% WO_x/TiO_2 catalyst showed two peaks at 580 °C and 770 °C which was assignable to WO_3 reduction [27]. H_2 consumption associated with WO_x reduction was 0.315 mmol/g. Undoped Pt/TiO_2 catalyst showed two Pt reduction peaks at -52 °C and -8 °C and the amount of H_2

consumption was 0.025 and 0.009 mmol/g respectively. The peak around 325 °C showed 0.018 mmol/g H_2 consumption. This peak was attributed to the reduction of the surface capping oxygen of TiO_2 [28, 29]. Theoretical H_2 consumption for 1 wt% Pt/TiO_2 was 0.05 mmol/g, which was calculated by assuming reduction of PtO_2 to metallic Pt. Compared to Pt/TiO_2 and WO_x/TiO_2 profile, H_2-TPR profile of WO_x-doped catalyst showed that Pt reduction peak was shifted to high temperature (26 °C) and WO_3 reduction peaks was shifted to lower temperature (600 °C). H_2 consumption amount in Pt reduction region was 0.011, 0.012, 0.020 and 0.040 mmol/g for 1, 5, 10, and 20 wt% WO_x respectively. The minor peak between 300- 400°C obtained in 5, 10 20 wt% WO_x containing catalyst with 0.004, 0.025 and 0.056 mmol/g H consumption respectively. In WO_x reduction region, H_2 consumption for 1, 5, 10, and 20 wt% WO_x was 0.152, 0.507, 0.701 and 0.280 mmol/g respectively. The shifting to lower temperature and increased H_2 consumption of WO_x suggested the presence of interactions between Pt and WO_x interactions.

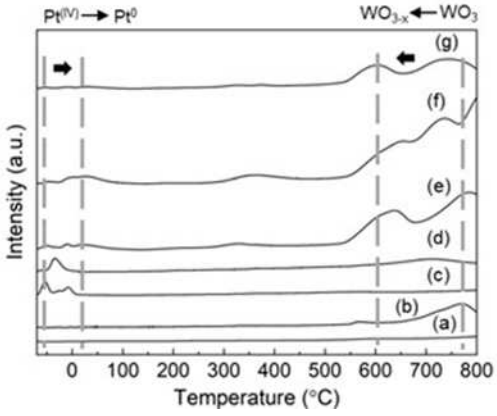

Fig. 3 H_2-TPR profile of TiO_2 (a), WO_x/TiO_2 (b), Pt/TiO_2 (c) Pt-1 wt% WO_x/TiO_2 (d), Pt-5 wt% WO_x/TiO_2 (e) Pt-10 wt% WO_x/TiO_2 (f) and Pt-20 wt% WO_x/TiO_2 (g)

CO uptake capacity analysis was conducted to evaluate the exposed Pt sites in undoped and WO_x-doped Pt/TiO_2 (Table S2). CO uptake capacity decreased significantly with increasing WO_x amount.

This phenomenon led to the formation of large Pt crystallite. Nevertheless, XRD analysis did not show Pt peak in all catalysts. The relationship between CO uptake and WO_x addition was investigated by He et al. [30]. When WO_x loading amount in Pt/TiO_2 catalyst was increased, the capacity of CO uptake was decreased. Low CO uptake of Pt-WO_x was attributed to WO_x overlayer formation on the surface of Pt metal. The formed WO_x overlayer may exhibit temperature-dependent mobility [31]. At low temperatures, this overlayer is relatively stable and suppresses H_2 adsorption, resulting in low initial catalytic activity. As the temperature increases (≥ 240 °C), WO_x species become increasingly mobile and can migrate from the Pt surface to the support. This migration exposes previously blocked Pt sites, leading to enhanced catalytic activity at elevated temperatures. However, this overlayer-migration mechanism cannot explain the observed catalytic activity at low temperatures.

In alternative interpretation, the decrease in CO uptake capacity was ascribed to strong metal-support interactions (SMSI) [31, 32]. These interactions lead to high W reduction. M'Boungou et al. revealed that low WO_x loading in $Pt–WO_x/Al_2O_3$ catalyst was made the catalyst difficult to reduce and catalytically inactive (Scheme 1) [33]. With high W loading, despite WO_x monolayer formation, a fraction of W species to migrate to Pt surface and was reduced to W^{4+}. The remaining major part of W species existed on support and remains as partially reduced (W^{5+}) in vicinity of Pt and non-reduced (W^{6+}) as bulk and dispersed tungsten bronzes. Our results showed consistency with these results. 1 wt% WO_x doped catalyst showed lower oxidation state (W^{4+}) was absent. In the case of high WO_x (5, 10, and 20 wt%) loading, lower oxidation state (W^{4+}) appeared, and its concentration increased with WO_x loading. However, high concentration of W^{4+} leads to competitive adsorption between NO and H_2. The moderate concentration of W^{4+} in 5 wt% WO_x catalyst allowed ammonia formation for above 175 °C.

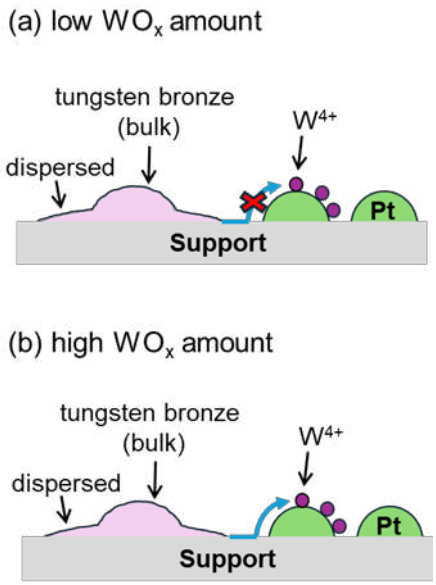

Scheme 1 Formation of W^{4+} over low (a) and high WO_x (b) loaded in Pt–WO_x catalyst

Fig. S3 shows NH_3-TPD profile of Pt/TiO_2 and WO_x-doped Pt/TiO_2. NH_3-TPD profile of Pt/TiO_2 catalyst showed two peaks at 179 °C and 278 °C. The total number of acidic sites was 0.046 mmol g^{-1} in the temperature range of 100 - 350 °C. In contrast, WO_x-doped Pt/TiO_2 showed a broad in the temperature range of 100 - 400 °C. Th acidic sites of 1 wt% WO_x, 5 wt% WO_x, 10 wt% WO_x and 20 wt% WO_x were 0.055, 0.049, 0.044 and 0.041 mmol g^{-1} respectively (Table S3). The acidity decreased with increased WO_x loading due to inactive W bulk formation. At this moment, the role of Brønsted and Lewis sites in NTA reaction is not clear. This will be a part of our future research.

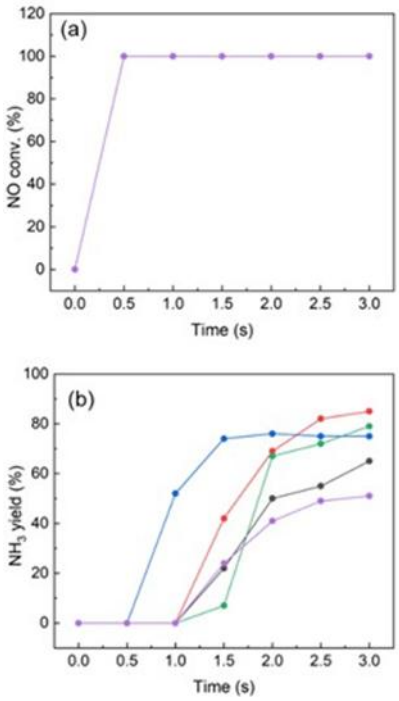

Fig. 4 Transient kinetic analysis for NO conversion (a) and NH_3 formation (b) using Pt/TiO_2 (black) Pt-1 wt% WO_x/TiO_2 (red), Pt-5 wt% WO_x/TiO_2 (blue) Pt-10 wt% WO_x/TiO_2 (green) and Pt-20 wt% WO_x/TiO_2 (purple) catalyst

To investigate H spillover in the bulk catalyst, transient kinetic experiments were performed under 0.1 % NO and 0.3 % H_2 in Ar at 150 °C. As shown in Fig 4a, NO conversion was unaffected by any of the catalysts. In case of NH_3 formation, Pt/TiO_2 showed NH_3 formation after 1 min. Comparing with NO conversion, NH_3 formation delayed, probably due to large amount of acid sites of support (TiO_2). Accelerated NH_3 formation over 1 and 5 wt% WO_x catalysts is suspected to be attributed to WO_x layer formation with covering acid sites. A large delay in NH_3 formation over 10 and 20 wt% WO_x catalysts observed. NH_3 yield after 2 seconds over 10 wt% WO_x catalyst was higher than 20 wt% WO_x, suggesting high capacity of H absorption for 20 wt%. H_{ad} concentration on metal surface decreased due to Had

migration into bulk and suppressed H-N formation reaction. From these results, we concluded that H spillover into WO_x bulk was presented and affected ammonia formation.

Conclusions

Undoped Pt/TiO_2 and WO_x-doped Pt/TiO_2 catalysts with varying loadings (1, 5, 10 and 20 wt%) were prepared via the impregnation method and evaluated for the nitrogen oxide to ammonia reaction in the temperature range of 100 °C to 500 °C. The catalytic performance was significantly influenced by WO_x loading. The catalyst with WO_x loading (5 wt%) exhibited the highest ammonia yield above 175 °C, including an optimal balance between hydrogen availability and W reducibility. Structural and surface analysis (XRD and XPS) confirmed tungsten bronzes formation upon reaction of WO_3 and H_2. H_2-TPR and CO chemisorption uptake capacity revealed strong metal-support interactions between Pt and WO_x, which enhance W reduction and the electronic environment of Pt. However, excessive WO_x loading (10–20 wt%) led to excessive hydrogen spillover into the WO_x bulk, reducing surface hydrogen availability and suppressing NH_3 formation at lower temperatures. A moderate WO_x content (5 wt%) resulted in a favorable concentration of W^{4+} species and sufficient surface hydrogen, enabling high ammonia selectivity in the mid-to-high temperature range. These findings provide valuable insights for designing advanced Pt-based catalysts with optimized WO_x promotion for NTA reaction.

Acknowledgements

This work is funded by MOONSHOT project and new energy and industrial technology development organization (JPNP18016).

Author Contributions

Chandan Chaudhari: Conceptualization, Experiments, Analysis and Paper writing, Yuichi Manaka: Analysis, supervision and paper writing, Tetsuya Nanba: supervision and paper writing

Funding

This work is funded by MOONSHOT project and new energy and industrial technology development organization (JPNP18016).

Data Availability

The results of this research can be obtained from the corresponding author upon a reasonable request.

Declarations

Competing Interests The authors declare no competing interests.

Ethical Approval Not applicable.

Consent to Participate Not applicable.

Consent for Publication All the authors have consented to the submission of the manuscript to this journal.

References

[1] Lewis AC (2021) Optimising air quality co-benefits in a hydrogen economy: a case for hydrogen-specific standards for NO_x emissions. Environ. Sci Atmos 1:201- 207. https://doi.org/10.1039/D1EA00037C

[2] Fowler D, Coyle M, Skiba U, Sutton MA, Cape JN, Reis S, Sheppard LJ, Jenkins A, Grizzetti B, Galloway JN, Vitousek P, Leach A, Bouwman AF, Butterbach-Bahl K, Dentener F, Stevenson D, Amann M, Voss M, (2013) The global nitrogen cycle in the twenty-first century Philos Trans Royal Soc B 368:1621. http://dx.doi.org/10.1098/rstb.2013.0164

[3] Boningari T, Smirniotis PG, (2016) Impact of nitrogen oxides on the environment and human health: Mn-based materials for the NO_x abatement Curr Opin Chem. Eng 13:133-141. https://doi.org/10.1016/j.coche.2016.09.004

[4] Metkar PS, Harold MP, Balakotaiah V, (2012) Selective catalytic reduction of NO_x on combined Fe- and Cu-zeolite monolithic catalysts: Sequential and dual layer configurations Appl Catal B 111-112:67-80. https://doi.org/10.1016/j.apcatb.2011.09.019

[5] Twigg MV, (2007) Progress and future challenges in controlling automotive exhaust gas emissions Appl Catal B 70:2-15. https://doi.org/10.1016/j.apcatb.2006.02.029

[6] Xue M, Lin BL, Tsunemi K, Minami K, Nanba T, Kawamoto T, (2021) Life cycle assessment of nitrogen circular economy-based NO_x treatment technology Sustainability 13: 7826. https://doi.org/10.3390/su13147826

[7] Kobayashi K, Atsumi R, Manaka Y, Matsumoto H, Nanba T, (2019) Effect of the TiO_2 crystal structure on the activity of TiO_2-supported platinum catalysts for ammonia synthesis via the NO–CO–H_2O reaction Catal Sci Technol 9:2898-2905. https://doi.org/10.1039/C9CY00061E

[8] Kobayashi K, Ogawa S, Matsumoto H, Matsuda K, Nanba T, (2020) Effect of Chemical and Physical Properties of Titanium Oxide Support Surface during Nitrogen Monoxide Reduction by Carbon Monoxide in Presence Water over Titanium Oxide Supported Platinum Catalyst J Jpn Petrol Inst 63: 28-37. https://doi.org/10.1627/jpi.63.28

[9] Chaudhari C, Manaka Y, Nanba T, (2024) Effect of TiO_2 Drying Conditions on the Catalytic Activity of Pt for Ammonia Synthesis from NO−H_2 ChemistrySelect 9: e202304789 https://doi.org/10.1002/slct.202304789

[10] Mergler YJ, Nieuwenhuys BF, (1997) Appl Catal B 12:95-110 NO reduction by H_2 over promoted Pt catalysts. https://doi.org/10.1016/S0926-3373(96)00068-9

[11] Nanba T, Meunier FC, Hardacre C, Breen JP, Burch R, Masukawa S, Uchisawa J, Obuchi A, (2008) Formation of ammonia during the NO-H_2 reaction over Pt/ZrO_2 J Phys Chem 2008, 112:18157-18163. https://doi.org/10.1021/jp8060812

[12] Adam EC, Skoglundh M, Folic M, Bendixen EV, Arielsson PG, Calesson PA, (2015) Ammonia formation over supported platinum and palladium catalysts Appl Catal B 165:10-19. https://doi.org/10.1016/j.apcatb.2014.09.064

[13] Yu Q, Richter M, Li L, Kong F, Wu G, Guan N, (2010) The promotional effect of Cr on catalytic activity of Pt/ZSM-35 for H_2-SCR in excess oxygen Catal Commun 11:955-959. https://doi.org/10.1016/j.catcom.2010.03.021

[14] Liu Z, Lu Y, Yuan L, Ma L, Zheng L, Zhang J, Huc T, (2016) Selective catalytic reduction of NOx with H_2 over WO_3 promoted Pt/TiO_2 catalyst Appl Catal B 188:189-197. https://doi.org/10.1016/j.apcatb.2016.02.008

[15] Shun K, Mori K, Masuda S, Hashimoto N, Hinuma Y, Kobayashi H, Yamashita H, (2022) Revealing hydrogen spillover pathways in reducible metal oxides Chem Sci 13:8137-8147. https://doi.org/10.1039/D2SC00871H

[16] Zeng Y, Jiang L, Zhang X, Xie S, Pei Y, Zhou G, Hua W, Qiao M, Li ZH, Zong B, (2022) Effect of titania polymorphs on the structure and catalytic performance of the Pt–WO_x/TiO_2 catalyst in glycerol hydrogenolysis to 1,3-Propanediol ACS Sustainable Chem Eng 10:9532-9545. https://doi.org/10.1021/acssuschemeng.2c02205

[17] Szilágyi IM, Fórizs B, Rosseler O, Szegedi Á, Németh P, Király P, Tárkány G, Vajna B, Varga-Josepovits K, László K, Tóth ÁL, Baranyai P, Leskelä M, (2012) WO_3 photocatalysts: Influence of structure and composition J Catal 294:119-127. https://doi.org/10.1016/j.jcat.2012.07.013

[18] Chen C, Lin G, Zhou W, Song H, Liang Y, Zhao W, Li J, Song W, Wang J, Li B Zhang Z, Fu J, (2025) H2 reduction-mediated reaction pathway switching in bimetallic Pt-WO_x catalyst: shifting fatty acid deoxygenation from decarboxylation to decarbonylation ACS J Catal 15:15211-15223. https://doi.org/10.1021/acscatal.5c041980

[19] So H, Lee J, Mahata C, Kim S, Kim S, (2024) Synaptic properties and short-term memory dynamics of TiO_2 /WO_x heterojunction memristor for reservoir computing Adv Mater Technol 9:2301390. https://doi.org/10.1002/admt.202301390

[20] Nakagawa Y, Hayashi, Y Yang S, Shibayama T, (2022) Effects of gas phase ion irradiation and vacuum annealing on the visible light photocatalytic properties of WO_3 Vacuum 206:111519. https://doi.org/10.1016/j.vacuum.2022.111519

[21] Chen J, Guo L, Zhu H, Qiu Y, Yin D, Zhang T, Chen J, Peng Y, Li J, (2021) Balancing redox and acidic properties for optimizing catalytic performance of SCR catalysts: A case study of nanopolyhedron CeO_x-supported WO_x J Environ Chem Eng 9:105828. https://doi.org/10.1016/j.jece.2021.105828

[22] Wang T, Hong Z, Sun F, Wang B, Jian C, Liu W, (2022) Interfacial engineering of tungstic disulfide–carbide heterojunction for high-current-density hydrogen evolution RSC Adv 12:27225-27229. https://doi.org/10.1039/D2RA04685G

[23] Zhu S, Gao X, Zhu Y, Li Y, (2015) Promoting effect of WO_x on selective hydrogenolysis of glycerol to 1,3-propanediol over bifunctional Pt–WO_x/Al_2O_3 catalysts J Mol Cat A Chem 398:391-398. https://doi.org/10.1016/j.molcata.2014.12.021

[24] Kuba S, Che M, Grasselli RK, Knözinger H, (2003) Evidence for the formation of W^{5+} centers and OH groups upon hydrogen reduction of platinum-promoted tungstated zirconia catalyst J Phy Chem B107:34593463. https://doi.org/10.1021/jp022313h

[25] Xi Y, Zhang Q, Cheng H, (2014) Mechanism of Hydrogen Spillover on WO_3(001) and Formation of H_xWO_3 (x = 0.125, 0.25, 0.375, and 0.5) J Phys Chem C 118:494-501. https://doi.org/10.1021/jp410244c

[26] Materer NF, Apblett A, Kadossov EB, Khan KR, Casper IV W, Hays K, Shams EF, (2016) The preparation and chemical reaction kinetics of tungsten bronze thin films and nitrobenzene with and without a catalyst Surf Sci 648:345-351. https://doi.org/10.1016/j.susc.2015.10.060

[27] Xiao X, Xiong S, Li B, Geng Y, Yang S, (2016) Role of WO_3 in NO reduction with NH_3 over V_2O_5-WO_3/TiO_2: A new insight from the kinetic study Catal Lett 146:2242-2251. https://doi.org/10.1007/s10562-016-1852-0

[28] Zhang C, Zhang C, He H, Tanaka, (2006) Catalytic performance and mechanism of a Pt/TiO_2 catalyst for the oxidation of formaldehyde at room temperature Appl Catal B 2006, 65:37-43. https://doi.org/10.1016/j.apcatb.2005.12.010

[29] Epling WS, Cheekatamarla PK, Lane AM, (2003) Reaction and surface characterization studies of titania-supported Co, Pt and Co/Pt catalysts for the selective oxidation of CO in H2-containing streams Chem Eng J 93:61-68. https://doi.org/10.1016/S1385-8947(02)00109-2

[30] He J, Burt SP, Ball M, Zhao D, Hermans I, Dumesic JA, Huber GW, (2018) Synthesis of 1,6-hexanediol from cellulose derived tetrahydrofuran-dimethanol with Pt-WO_x/TiO_2 catalysts ACS Catal 8:1427-1439. https://doi.org/10.1021/acscatal.7b03593

[30] Pallares-García A, Contreras JL, Pérez-Cabrera J, Zeifert B, Vázquez T, Salmones J, Gutiérrez-Limón MA, (2021) Stabilization of Pt in SiO_2–$Al2O_3$ microspheres at high

mechanical resistance, promoted with W oxides for the combustion of CO Catalysts, 2021, 11, 1320. https://doi.org/10.3390/catal11111320

[31] Park S, Liu Z, Gorte RJ, Vohs JM, (2026) Evidence for the mobility of tungsten oxide overlayers on supported Pt catalysts Appl. Catal B-Environ Energy 382:125971. https://doi.org/10.1016/j.apcatb.2025.125971

[32] Regalbuto JR, Fleisch TH, Wolf EE, (1987) An integrated study of Pt/WO3/SiO2 catalysts for the NO-CO reaction: I. catalyst characterization by XRD, chemisorption, and XPS J Catal 107:114-128. https://doi.org/10.1016/0021-9517(87)90277-6

[33] M'Boungou JS, Hilaire L, Maire G, Garin F, (1991) Catal Lett 10:401-411. https://doi.org/10.1007/BF00769175

Fig. 1 Effect of temperature on NO conversion (a) and NH_3 formation (b) over undoped Pt/TiO_2 (■), Pt-1 wt% WO_x/TiO_2 (▲), Pt-5 wt% WO_x/TiO_2 (●), Pt-10 wt% WO_x/TiO_2 (▼), Pt-20 wt% WOx/TiO_2

Fig. 2 XRD analysis of commercial WO_3 (a) and reduced catalysts; Pt/TiO_2 (b), Pt-1 wt% WO_x/TiO_2 (c), Pt-5 wt% WO_x/TiO_2 (d) Pt-10 wt% WO_x/TiO_2 (e) and Pt-20 wt% WO_x/TiO_2 (f). Abbreviation: A, anatase; R, rutile; W, WO_3

Fig. 3 H_2-TPR profile of TiO_2 (a), WO_x/TiO_2 (b), Pt/TiO_2 (c) Pt-1 wt% WO_x/TiO_2 (d), Pt-5 wt% WO_x/TiO_2 (e) Pt-10 wt% WO_x/TiO_2 (f) and Pt-20 wt% WO_x/TiO_2 (g)

Fig. 4 Transient kinetic analysis for NO conversion (a) and NH_3 formation (b) using Pt/TiO_2 (black) Pt-1 wt% WO_x/TiO_2 (red), Pt-5 wt% WO_x/TiO_2 (blue) Pt-10 wt% WO_x/TiO_2 (green) and Pt-20 wt% WO_x/TiO_2 (purple) catalyst

Graphical abstract

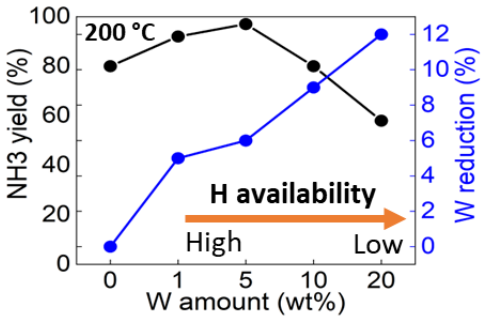

Supplementary Files

This is a list of supplementary files associated with this preprint. Click to download.

- SI6.docx